Heliyon 9 (2023) e15645

Contents lists available at ScienceDirect

Heliyon

journal homepage: www.cell.com/heliyon

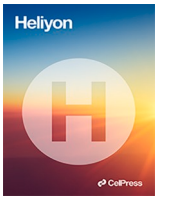

Research article

Effect and mechanism of Tangzhiqing in improving cardiac function in mice with hyperlipidaemia complicated with myocardial ischaemia

Zhihui Song [a,1], Rui Chen [b,1], Caijun Wang [a], Guiyun Pan [a], An Yan [a], Guinan Xie [a], Zhihua Yang [a], Wanying Feng [a], Yi Wang [a,*]

[a] Institute of Traditional Chinese Medicine, Tianjin University of Traditional Chinese Medicine, Tianjin, 301617, China
[b] College of Traditional Chinese Medicine, Tianjin University of Traditional Chinese Medicine, Tianjin, 300193, China

ARTICLE INFO

Keywords:
Tangzhiqing
Network analysis
Hyperlipidaemia
Myocardial ischaemia
PI3K/AKT
Apoptosis

ABSTRACT

Purpose: Tangzhiqing formula (TZQ) is a traditional Chinese medicine prescribed to treat lipid metabolism disorders, atherosclerosis, diabetes and diabetic cardiomyopathy. However, some challenges and hurdles remain. TZQ showed promising results in treating diabetes and hyperlipidaemia. However, its effect on and mechanism of action in hyperlipidaemia complicated with myocardial ischaemia (HL-MI) remain unknown.

Methods: In this study, a network pharmacology-based strategy integrating target prediction was adopted to predict the targets of TZQ relevant to the treatment of HL-MI and to further explore the involved pharmacological mechanisms.

Results: A total of 104 potential therapeutic targets were obtained, including MMP9, Bcl-2, and Bax, which may be related to the apoptosis and PI3K/AKT signalling pathways. Then, we confirmed these potential targets and pathways with animal experimentation. TZQ reduced lipid levels, increased the expression levels of Bcl-2, decreased Bax, caspase-3 and caspase-9 expression levels, and activated the PI3K/AKT signalling pathway.

Conclusion: In conclusion, this study provides new insights into the protective mechanisms of TZQ against HL-MI through network pharmacology and pharmacological approaches.

1. Introduction

Cardiovascular disease (CVD) is one of the leading causes of mortality worldwide [1,2] and myocardial ischaemia refers to a type of ischaemic cardiomyopathy that is a primary cause of death from CVD [3]. Hyperlipidaemia is a metabolic disease characterized by

Abbreviations: CVD, cardiovascular disease; CAT, catalase; DL, drug-like; FFA, free fatty acid; HDL-C, high-density lipoprotein cholesterol; IVS, interventricular septum thickness; GPx, glutathione peroxidase; LDL-C, low-density lipoprotein cholesterol; LVEF or EF, left ventricular ejection fraction; LVFS or FS, left ventricular short axis shortening rate; LVPW, left ventricular posterior wall thickness; LVID, left ventricular inner diameter; MDA, malondialdehyde; OB, oral bioavailability; SOD, superoxide dismutase; TZQ, Tangzhiqing; TC, total cholesterol; TG, triglycerides; TCM, traditional Chinese medicine; TCMSP, traditional Chinese medicine systems pharmacology database.

* Corresponding author. Tianjin University of Traditional Chinese Medicine, #10 Poyanghu Road, West Area, Tuanbo New Town, Jinghai District, Tianjin, 301617, China.
E-mail address: wangyi@tjutcm.edu.cn (Y. Wang).

[1] The first two authors contributed equally to this work.

https://doi.org/10.1016/j.heliyon.2023.e15645
Received 1 August 2022; Received in revised form 13 April 2023; Accepted 17 April 2023
Available online 20 April 2023

elevated plasma levels of triglycerides (TG), low-density lipoprotein cholesterol (LDL-C), and total cholesterol TC (total cholesterol) [4].

Hyperlipidaemia not only impairs cardiac function by accelerating the progression of atherosclerosis but also has a significant role in heart contractile function and electrophysiological responsiveness [5]. PI3K/AKT is an important signalling pathway for cell growth. It can affect the survival, proliferation and apoptosis of cardiomyocytes, impact the energy metabolism and regulation of cardiomyocytes, and improve blood lipid metabolism and regulate blood sugar, which is closely related to the regulation of cardiomyocyte function [6].

To improve the survival rate of cardiovascular patients, drugs or surgical treatment can be selected. Nitrates are the preferred drugs against myocardial ischaemia, as they can quickly relieve symptoms by reducing myocardial oxygen consumption, relaxing the coronary artery to relieve spasm, improving subendocardial blood supply and relaxing blood vessels. There are many side effects and adverse reactions associated with these medications, such as facial flushing, lowering of blood pressure, headaches, and drug resistance. These adverse effects can easily undermine the therapeutic effects of these drugs. Traditional Chinese Medicine (TCM) has the advantages of being a multicomponent and multitarget treatment and has low toxicity and few side effects [7,8].

TZQ is a common clinical prescription used by academician Boli Zhang for the treatment of hyperlipidaemia, diabetes and coronary heart disease. TZQ is composed of *Morus alba* L. *(mulberry leaves), Nelumbo nucifera Gaertn (*lotus leaves*), Crataegus pinnatifida Bunge* var. *major N. E. Br* (hawthorn leaves), the root of Salvia miltiorrhiza Bunge *(Salvia miltiorrhiza Bunge*), and the air-dried root of Paeonia lactiflora Pall (red peony). In a chemical and metabolic component analysis of TZQ dynamics, 86 absorbed components and 48 metabolites were found in rat plasma, urine, and faeces. Alkaloids and flavonoids are the primary absorbed components, and glucuronides and sulfates are the primary metabolites [9]. TZQ has the effects of reducing turbidity, removing blood stasis and eliminating rupidium [10]. Modern pharmacological studies have shown that TZQ can reduce hyperinsulinaemia, hyperglycaemia and obesity by regulating adipocyte differentiation and insulin action [11]. It can also prevent prediabetes by increasing the role of the IRS-1-dependent signalling pathway in muscle [12]. Moreover, TZQ has the effect of resisting myocardial cell apoptosis in diabetic rats. A possible mechanism of action for this effect was increasing the expression of Bcl-2, thereby reducing the ratio of Bax/Bcl-2 and inhibiting cardiomyocyte apoptosis [13]. In addition, our research group has already shown that TZQ attenuated the formation of atherosclerotic lesions and pyroptosis in the aortic intima of high-fat diet-fed ApoE−/− mice. We revealed that TZQ regulates arachidonic acid metabolism, glycerophospholipid metabolism, steroid hormone biosynthesis, and unsaturated fatty acid biosynthesis, all of which have antiatherosclerotic effects [14].

However, the effect and mechanism of action of TZQ on myocardial ischaemia are still unclear, which is the focus of this study.

Network analysis is based on the joint development of bioinformatics, systems biology and multipharmacological approaches [15]. Its ability to describe the complexity between biological systems, drugs and diseases from a network perspective is quite similar to the overall concept of TCM [16]. This research utilized network pharmacology and experimental data to investigate the effect and mechanism of action of TZQ on cardiac function in HL-MI mice (Fig. 1).

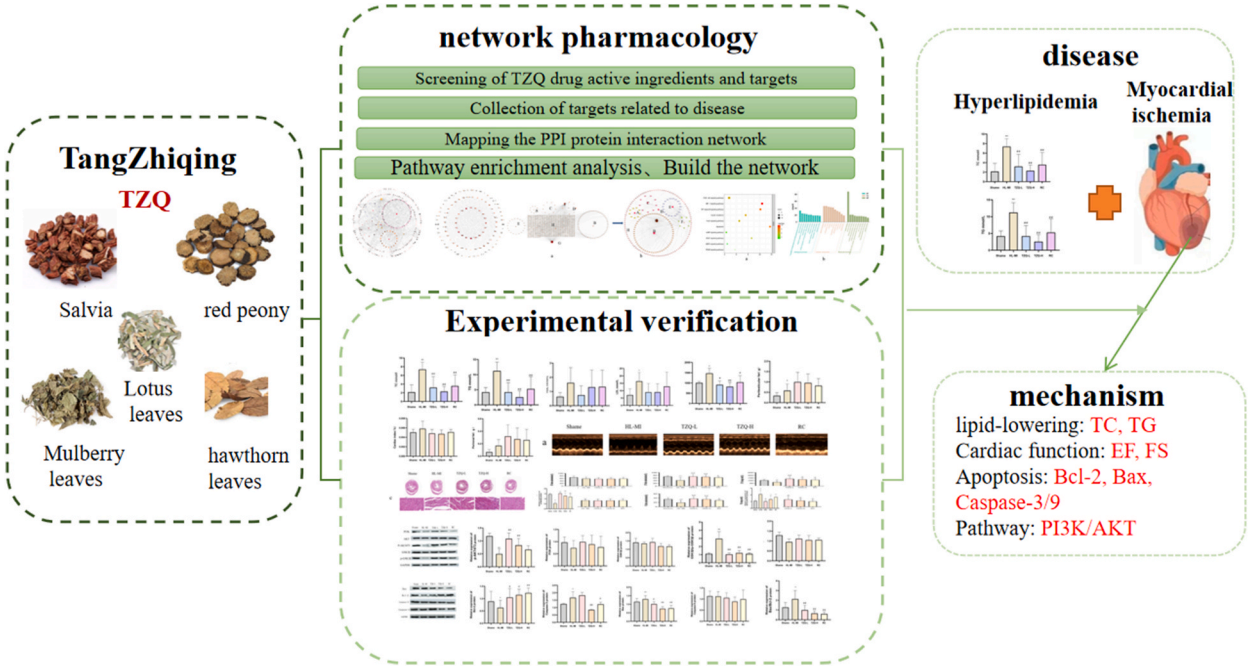

Fig. 1. Graphical abstract.

2. Methods and materials

2.1. Target acquisition

2.1.1. Tangzhiqing compound database construction

To discover the targets of TZQ, we used the TCMSP database (https://old.tcmsp-e.com/tcmsp.php), and the effective compounds were screened according to an oral bioavailability (OB) greater than or equal to 30% and a drug-like property (DL) greater than or equal to 0.18 [17]. Additionally, the two-dimensional/three-dimensional (2D/3D) structures and PubChem IDs of compounds were calibrated using PubChem. Then, the possible targets of the effective components were matched by the UniProt database (https://www.uniprot.org/).

2.1.2. Screening of HL-MI-related proteins and predicted target proteins

HL-MI-related protein targets were screened using the OMIM (https://omim.org/), GeneCards (https://www.genecards.org/) and DisGeNET (https://academic.oup.com/nar/article/45/D1/D833/2290909) databases, and common targets were selected as candidate targets for HL-MI. Then, the candidate and predicted targets were validated by their unique UniProtKB IDs and target names in the UniProt (https://www.UniProt.org/) database, and the final HL-MI targets were identified. Finally, the targets of TZQ and the targets of HL-MI were intersected to obtain the potential targets of TZQ in treating HL-MI.

2.2. Network construction

To further explore the relationship among TZQ, hyperlipidaemia and myocardial ischaemia, the intersecting targets of the three categories were selected to make a PPI network in Cytoscape 3.8.2. DAVID (https://david.ncifcrf.gov/) was used to predict KEGG pathways and explain biological functions, and putative proteins with $P \leq 0.01$ were considered significantly related.

2.3. Further validation of the targets

2.3.1. Preparation of drugs

TZQ was provided by the Department of Pharmacy, Institute of Traditional Chinese Medicine, Tianjin University of Traditional Chinese Medicine. After soaking the above five traditional Chinese medicines in water, they were decocted twice, filtered, and combined; the filtrate was concentrated into a thick paste, dried under reduced pressure, and crushed into a powder. The drug ratio of the ointment was as follows: hawthorn leaves, 6.25%; mulberry leaves and lotus leaves, 19.75%; Salvia miltiorrhizae, 4.7%; and red peony, 6.3%. TZQ was found to contain lotus alkaloid, paeoniflorin, salvianolic acid B, hypericin, and rutin (6.40, 1.75, 1.70, 0.004, and 0.006 mg, respectively) [18]. Rosuvastatin calcium tablet (RC) (Batch no. HJ20160545) was produced by Pfizer Inc. (New York, NY, USA).

2.3.2. Hyperlipidaemia complicated with the HL-MI model

SPF 8-week-old male C57BL/6J mice, weighing 20 ± 2 g, were purchased from SiPeiFu (Beijing Biotechnology), with the certificate number SCXK (Beijing) 2019-0010. These mice were raised in the Animal Center of Tianjin University of Traditional Chinese Medicine (TCM–LAEC2021037). All experimental protocols were conducted in accordance with the guidelines approved by the Animal Care Committee of Tianjin University of Traditional Chinese Medicine and the Animal Ethics Committee of Tianjin University of Traditional Chinese Medicine (TCM–LAEC2021037). Except for the sham group, all animals were fed high-fat feed for 20 weeks (MD12015A, Medicience, China) after one week of adaptive feeding. After establishing the hyperlipidaemic model, this method was determined to

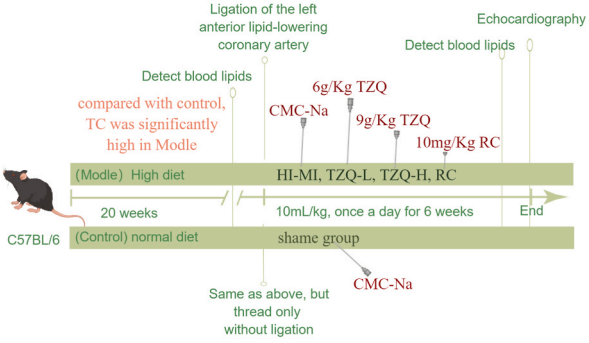

Fig. 2. Animal modelling, grouping, and drug administration. Sham operation group (sham) (n = 13): common feed + 0.5% carboxymethylcellulose sodium ([CMC–Na]) solution 0.1. HL-MI model group (n = 13): high-fat feed + 0.5% CMC–Na solution. TZQ-L group (n = 13): high-fat feed + 6 g/kg TZQ. TZQ-H group (n = 13): high-fat feed + 9 g/kg TZQ. Rosuvastatin group (RC) (n = 13): high-fat feed + 10 mg/kg rosuvastatin. TZQ and RC were made into a powder, and 0.5% CMC-Na was used as the solvent to prepare different concentrations of drug solutions. Each group was administered comparable medicines at a dose of 10 mL/kg once a day for 6 weeks.

be successful. To create a myocardial ischaemic model, we ligated the left anterior descending coronary artery of mice. In addition, a small animal ultrasound (Vevo2100, FUJIFILM VisualSonics, Canada) test was conducted to determine the reliability of the model. The mice were randomly assigned to five groups based on the left ventricular ejection fraction and body weight (Fig. 2).

2.4. Pharmacodynamics

LVEF and left ventricular short axis shortening rate (LVFS) were measured with a small animal ultrasonic instrument (Vevo3100, FUJIFILM VisualSonics, Canada). The morphology of cardiac pathology was assessed based on haematoxylin-eosin (HE) staining (G1120, Solarbio), and TC, TG, HDL-C (high-density lipoprotein cholesterol) and LDL-C levels were measured using kits purchased from Nanjing Jiancheng Bioengineering Research Institute. The FFA content in mouse serum was measured, and an FFA ELISA kit was purchased from Biotopped Life Sciences.

2.5. Haematoxylin-eosin staining

Aortic tissue was fixed in 4% paraformaldehyde and then embedded in paraffin, and paraffin sections (5 μm) were cut and mounted

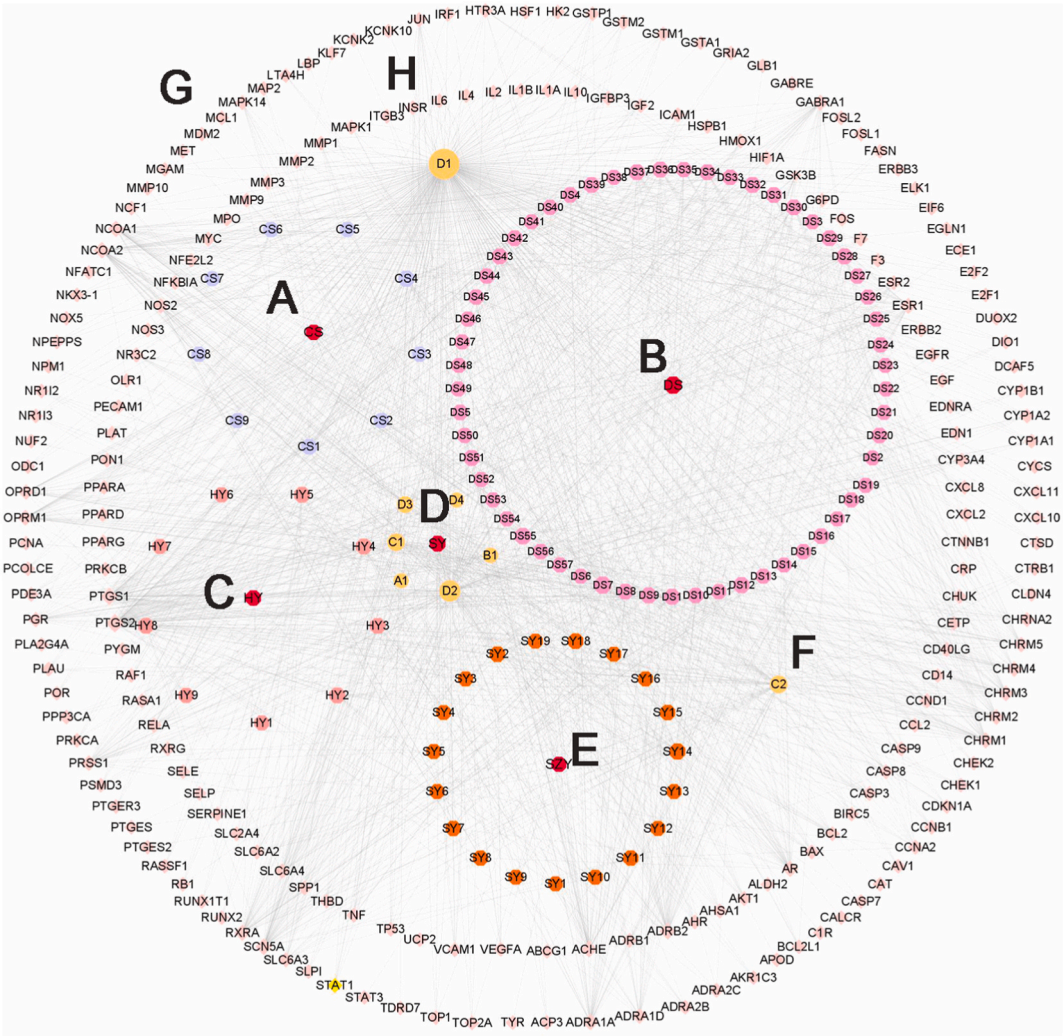

Fig. 3. Potential active ingredients and gene targets of TZQ. A. The red octagon marked with CS: Radix Paeoniae Rubra. B. The red octagon marked with DS: Salvia miltiorrhiza. C. The red octagon marked with HY: lotus leaf. D. The red octagon marked with SY: hawthorn leaves. E. The red octagon marked with SZY: mulberry leaves. F. The orange–yellow oval: overlapping compounds between drugs. G. The outermost ring is a pink diamond: noncore target. H. The penultimate pink diamond: core target. Red (A, B, C, D, E) represents drugs in TZQ; pink (G, H) represents TZQ gene targets. The rose-pink octagon represents the effective compounds of DS. The dark pink octagon represents HY effective compounds. The orange–yellow oval represents SY active compounds. The purple octagon represents CS active compounds. (For interpretation of the references to colour in this figure legend, the reader is referred to the Web version of this article.)

on glass slides for HE staining.

2.6. Western blot

Heart tissues were extracted with RIPA (CW2333S, CWBIO) lysate containing a phosphatase inhibitor and PMSF mixture (P0100, Solarbio). After quantitative analysis by a BCA protein quantitative kit (PC0020, Beijing, Solarbio), RIPA lysate and protein loading buffer were added in proportion and frozen for later use. After loading, electrophoresis, membrane transfer, blocking, incubation with primary antibody and peroxidase-conjugated secondary antibody, the bands were visualized by enhanced chemiluminescence (ECL, Millipore). ImageJ was used to analyse the optical density of each band. The details of the primary antibodies used were as follows: PI3K (1:2000 dilution, Wanleibio, Cat. No. WL02240), AKT (1:1000 dilution, CST, Cat. No. 4685s), p-AKT473 (1:1000 dilution, CST, Cat. No. 4685s), GSK3β (1:1000 dilution, CST, Cat. No. 12456T), p-GSK3β (1:1000 dilution, Boster, Cat. No. D5C5Z), Bax (1:1000, Abcam, Cat. No. ab182733), Bcl-2 (1:1000 dilution, Abcam, Cat. No. ab196495), caspase-3 (1:2000 dilution, Abcam, Cat. No. ab184787), caspase-9 (1:1000 dilution, Abcam, Cat. No. ab184786), and goat anti-rabbit IgG (1:10,000 dilution, Abcam, Cat. No. ab6721).

2.7. Statistical analysis

Each experiment was carried out independently three times, and the data are expressed as the mean ± standard deviation. SPSS23.0 (Chicago, Illinois, USA) was used for statistical analysis. The measurement data are expressed as the mean ± standard deviation and were analyzed by one-way analysis of variance (ANOVA). The enumeration data were analyzed by the chi-square test. $P < 0.05$ was considered statistically significant. GraphPad Prism 8.0 software was used to process and graph data.

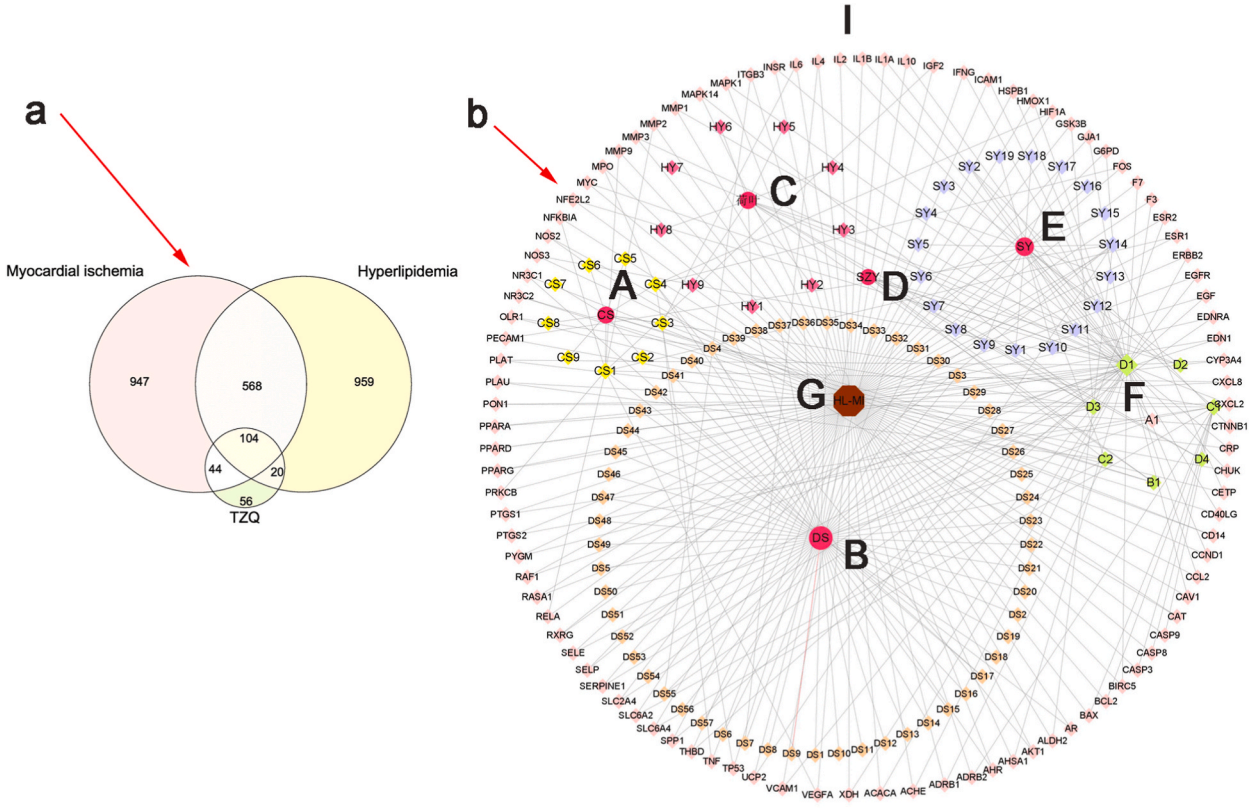

Fig. 4. Determination of repetitive targets related to TZQ and HL-MI. A. TZQ-hyperlipidaemia-myocardial ischaemia Venn diagram. B. The intersection target map of the effective compound component of TZQ-hyperlipidaemia-myocardial ischaemia. A. The red oval marked with CS: radix paeoniae rubra. B. The red oval marked with DS: Salvia miltiorrhiza. C. The red oval marked with HY: lotus leaf. D. The red oval marked with SZY: hawthorn leaves. E. The red oval marked with SY: mulberry leaves. F. (A1 and bright green diamond: overlapping compounds between drugs. G. The dark red octagonal marked with HL-MI: Disease: hyperlipidaemia with myocardial ischaemia; H: target. Red (A, B, C, D, E) represents drugs in TZQ. I. The pink diamond represents a common target of TZQ and hyperlipidaemia and myocardial ischaemia. The orange diamond represents the effective compounds of DS. The dark pink diamond represents HY effective compounds. The purple diamond represents SY active compounds. The bright yellow diamond represents CS active compounds. (For interpretation of the references to colour in this figure legend, the reader is referred to the Web version of this article.)

3. Results

3.1. Network analysis

3.1.1. Potential active ingredients and gene targets of TZQ

The TCMSP database was used to search for the effective components of TZQ prescription, and the possible targets of effective compounds were matched through the UniProt database. TZQ consists of five medicines, with 143 effective compounds and 225 targets (Fig. 3) (Supplementary Tables 1, 2 and 3).

3.1.2. Intersecting targets of TZQ and HL-MI

To explore the relationship among TZQ, myocardial ischaemia and hyperlipidaemia, a structural diagram of the targets of TZQ, hyperlipidaemia and myocardial ischaemia was made (Fig. 4). Finally, 104 intersecting genes were identified, including Bax, Bcl-2, caspase-3, TNF, and MMP9 (Fig. 4).

3.1.3. PPI network analysis and biological enrichment analysis of common targets

To explore the mechanism of action of TZQ in treating HL-MI, we constructed a drug-disease target PPI network (Fig. 5). There were 104 intersecting targets of TZQ-hyperlipidaemia-myocardial ischaemia. According to the degree value, the network diagram revealed 49 targets with a degree less than 30, 35 targets with a degree greater than 30 and less than 60, and 20 targets with a degree greater than 60. The target proteins are mainly involved in inflammation, apoptosis and oxidative stress.

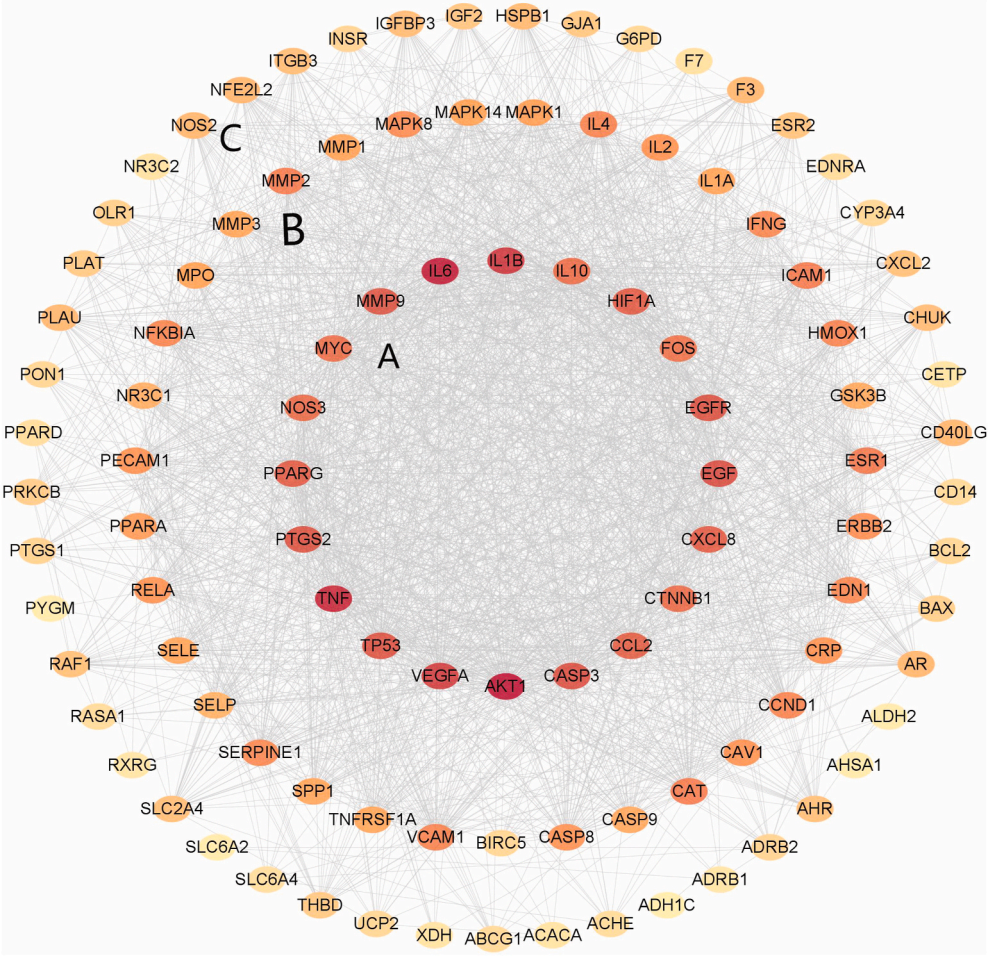

Fig. 5. PPI network analysis and biological enrichment analysis of common targets. A. The first circle is a dark yellow oval: core target, with a degree value above 61. B. The second circle is an orange oval: core target, with a degree value of 31–60. C. The outermost circle is a light yellow oval: core target, with degree value of 1–30. (For interpretation of the references to colour in this figure legend, the reader is referred to the Web version of this article.)

3.1.4. GO function annotation and KEGG pathway analysis

To further explore the mechanism of TZQ in the treatment of HL-MI, we selected 104 targets at the intersection of drug and disease for KEGG enrichment analysis of related pathways and GO functional annotation. A total of 105 pathways were enriched in the 104 targets. According to the count value, the top ten pathways were selected to make a histogram (Fig. 6a). The top ranked signalling pathways included those of PI3K/AKT, HIF-1, NF-κB, and FOXO. The GO functional analysis is mainly reflected in three levels: BP, CC and MF (Fig. 6b). The BPs mainly involve inflammation, apoptosis, hypoxia, and lipopolysaccharide-mediated signalling pathways. The CCs mainly include mitochondria, nucleus, and plasma membrane. The MFs mainly include enzyme binding, protein binding, and cytokine activity.

3.1.5. HL-MI related target-drug-active ingredient map

Based on the above results, to observe the possible mechanism of action of TZQ on HL-MI more intuitively, we drew a pathway-target-disease-network diagram (Fig. 7).

3.2. Animal experiments

3.2.1. Changes in body weight and fat distribution

Compared with mice in the sham group, mice in the model group were listless, had greasy hair, were light weight, had rickets, had less perirenal fat and peritesticular fat, and had a high heart index (Fig. 8a, b, c). Compared with the HL-MI group, mice in the TZQ-L and TZQ-H groups had a normal mental state, drier hair, more perirenal fat and peritesticular fat, and a lower heart index (Fig. 8a, b, c).

3.2.2. TZQ reduces blood lipids in HL-MI mice

To determine the effect of TZQ on blood lipids in mice, the levels of TC (Fig. 9a), TGs (Fig. 9b), LDL-C (Fig. 9e), and HDL-C (Fig. 9d) in liver tissue homogenate and free fatty acids (FFAs) (Fig. 9c) in serum were detected. The results showed that compared with those in the sham group, the concentrations of TC, TGs and FFAs in mice in the model group were significantly increased ($p < 0.01$). The concentrations of LDL-C and HDL-C were increased, but the differences were not statistically significant. Compared with those in mice in the model group, the concentrations of TC, TGs and FFAs in mice in the TZQ-L and TZQ-H groups were significantly decreased ($p < 0.01$). The concentrations of LDL-C and HDL-C were decreased but were not significantly reduced.

Liver HE staining (Fig. 9f) showed that the liver tissue structure of mice in the sham group was clear, the cell morphology was normal, and the liver cells radiated around the central lobular vein. In the model group, hepatic steatosis occurred, liver cells were arranged loosely, the cell volume became enlarged, the cells were rounded, and there were lipid droplets of different sizes and numbers in the cytoplasm. In the TZQ treatment group, the number of vacuolar changes in the liver tissue was significantly reduced, and the cell arrangement was normal. These results indicate that TZQ can reduce blood lipid levels in mice with HL-MI.

3.2.3. TZQ improves cardiac function in HL-MI mice

M-mode echocardiography was performed 6 weeks after myocardial ischaemia modelling and administration (Fig. 10a). Before group dosing, no difference in EF and FS between model groups (Fig. 10b and e). In the sham group, the left ventricle diameter was normal, the thickness of the left ventricle wall was uniform, and the movement was regular. Compared with those in the sham group,

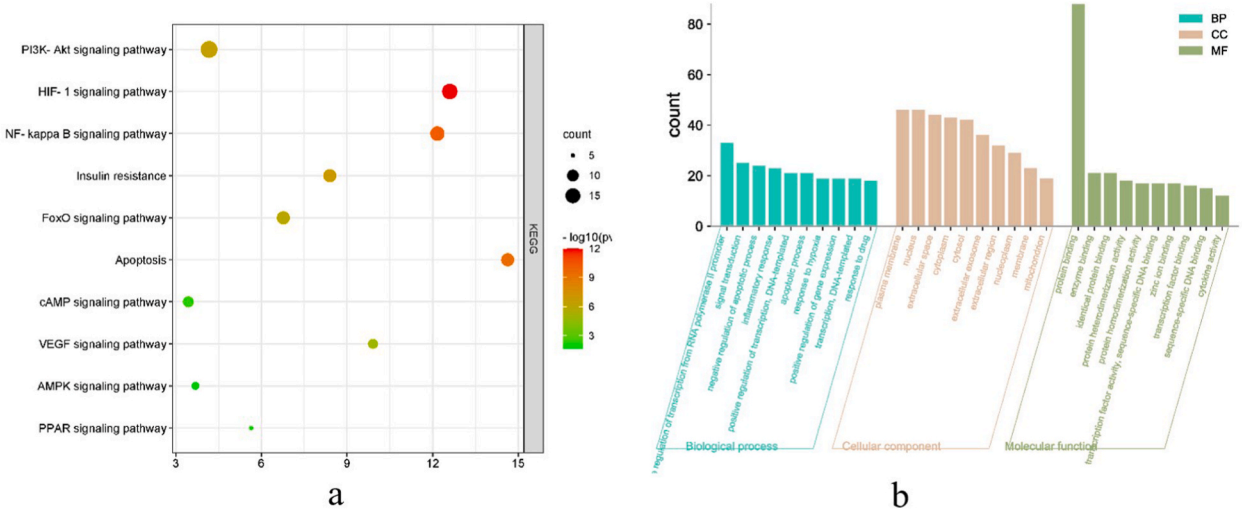

Fig. 6. KEGG signalling pathway and GO function notes. A. KEGG signalling pathway (the higher the position and the darker the colour is, the stronger the confidence. B. GO function notes. BP (blue histogram) represents biological process, CC (pink histogram) represents cellular components, and MF (green histogram) represents molecular function.

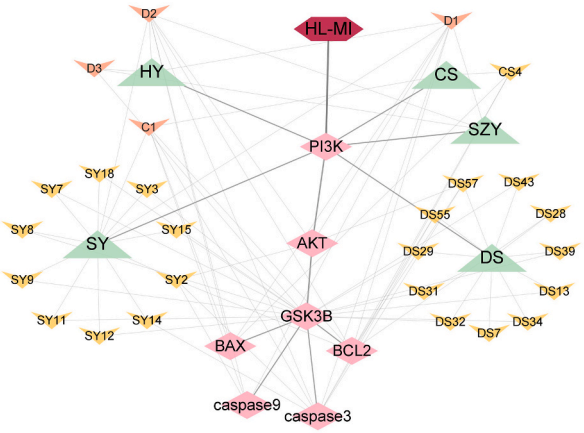

Fig. 7. HL-MI related target-drug-active ingredient map. A dark pink hexagon indicates HL-MI for disease. The pink diamond represents possible pathway targets. Orange represents the active ingredient of the drug. The green triangle represents TZQ prescription.

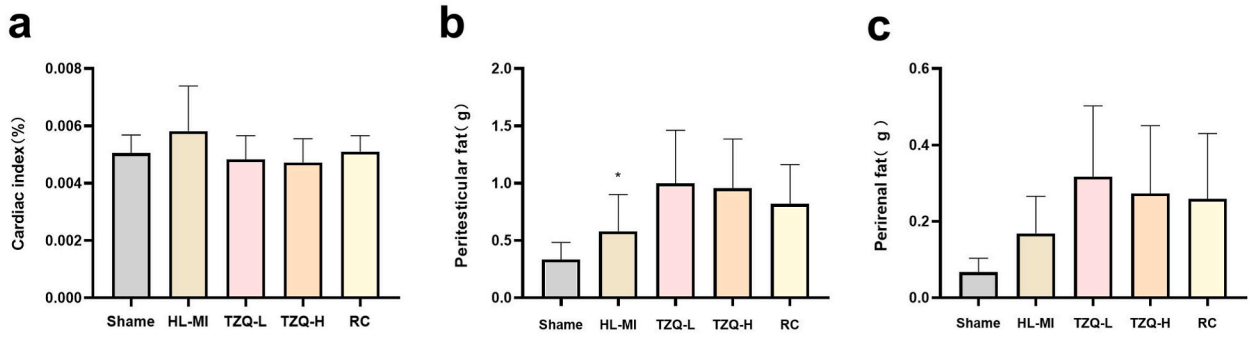

Fig. 8. Changes in body weight and fat distribution (n = 6). A. Heart index of mice: heart weight/body weight. B. Perirenal fat. C. Peritesticular fat. Sham: sham surgery group; HL-MI: model group; TZQ-L: TZQ 6 g/kg group; TZQ-H: TZQ 9 g/kg group; and RC: rosuvastatin 10 mg/kg group. *P < 0.05, **P < 0.01 (compared with sham), $^{\#}P < 0.05$, $^{\#\#}P < 0.01$ (compared with HL-MI).

left ventricular dilation was significantly increased, the anterior wall was thinner, the posterior wall was thicker, and movement was weakened in the model group. Compared with those in the model group, the left ventricular thickness was uniform, and the movement was regular in the TZQ treatment group.

To explore whether TZQ can improve the cardiac function of HL-MI mice, we used echocardiography to detect LVEF and LVFS. Compared with those in the sham group, LVEF (Fig. 10c), LVFS (Fig. 10f). EF change rate (Fig. 10d) and FS change rate (Fig. 10g) were significantly decreased in the model group (P < 0.01). Compared with those in the model group, LVEF (Fig. 10c), LVFS (Fig. 10f), EF change rate (Fig. 10d) and FS change rate (Fig. 10g) were significantly increased in the TZQ-L and TZQ-H groups (P < 0.01).

HE staining of the heart (Fig. 10h) showed that the nuclei of the myocardium of mice in the sham group were blue, the myocardium cells were neatly arranged, the muscle bundles were full, and the cytoplasm was bright red. Compared with that of the sham group, the myocardium of the model group was disordered with inflammatory cell infiltration and ventricular damage. Compared with that in the model group, the appearance of cardiomyocytes in the TZQ-L and TZQ-H groups was normal, inflammatory cell infiltration was significantly reduced, and cardiomyocytes were arranged neatly. These results indicate that TZQ improves cardiac function in HL-MI.

3.2.4. TZQ improves cardiac function in HL-MI mice by activating the PI3K/AKT signalling pathway

The effect of TZQ on the expression of PI3K/AKT signalling pathway-related proteins in the heart tissue of HL-MI mice was explored (Fig. 11a). The expression levels of PI3K (Fig. 11b), AKT (Fig. 11c), p-AKT473 (Fig. 11e), GSK3β (Fig. 11d) and p-GSK3β (Fig. 11f) in the myocardial tissue of HL-MI mice were detected by WB. Compared with those in the sham group, the expression levels of the PI3K, AKT, and GSK3β proteins in the model group were decreased (the difference was not statistically significant). The expression levels of the p-AKT473 and p-GSK3β proteins in the model group were decreased ($p < 0.01$), and the ratios of AKT/p-AKT473 and GSK3β/p-GSK3β were greatly increased. Compared with those levels in the model group, the expression levels of the p-AKT473 and p-GSK3β proteins in the TZQ-L and TZQ-H groups were significantly increased ($p < 0.01$), and the ratio of AKT/p-AKT473 and GSK3β/p-GSK3β were markedly decreased.

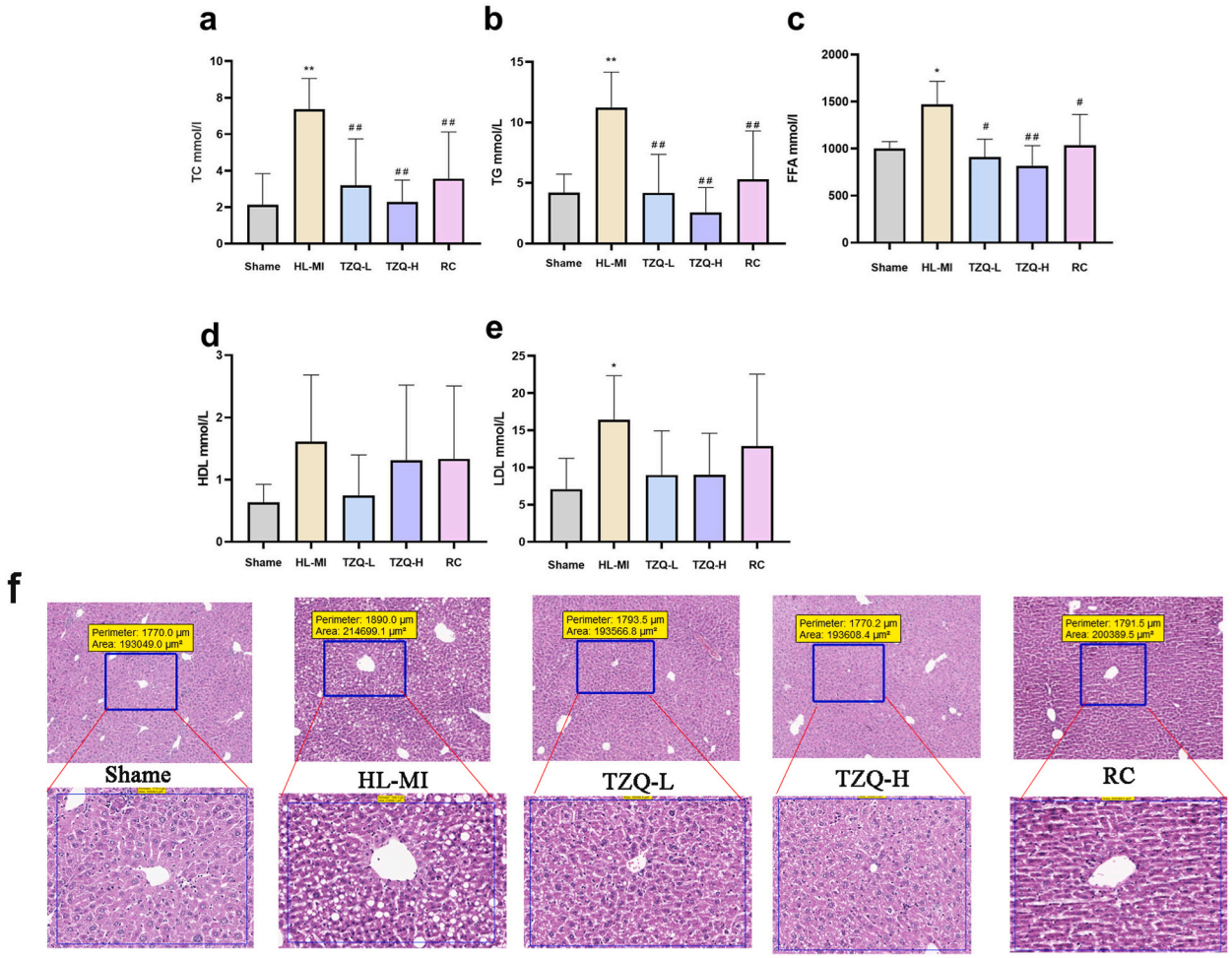

Fig. 9. TZQ reduces blood lipid levels in HL-MI mice. A. The levels of TC in the liver tissue homogenate **(n = 6)**. B. The levels of TGs in the liver tissue homogenate **(n = 6)**. D. The levels of LDL-C in the liver tissue homogenate **(n = 6)**. E. The levels of HDL-C in the liver tissue homogenate **(n = 6)**. C. The levels of FFAs in serum **(n = 6)**. F. Liver HE staining **(n = 3)**. Sham: sham surgery group; HL-MI: model group; TZQ-L: TZQ 6 g/kg group; TZQ-H: TZQ 9 g/kg group; and RC: rosuvastatin 10 mg/kg group. *P < 0.05, **P < 0.01 (compared with sham), $^{\#}P < 0.05$, $^{\#\#}P < 0.01$ (compared with HL-MI).

3.2.5. TZQ improves cardiac function in HL-MI mice by inhibiting apoptosis

To explore the effect of TZQ on the expression of apoptosis-related proteins in the cardiac tissue of HL-MI mice, the expression levels of Bcl-2 (Fig. 12b), Bax (Fig. 12c), Bax/Bcl-2 (Fig. 12e), caspase-3 (Fig. 12d) and caspase-9 (Fig. 12f) in the myocardial tissue of HL-MI mice were detected by WB (Fig. 12a). Compared with the levels in the sham group, the expression level of the antiapoptotic factor Bcl-2 was decreased, the expression level of the proapoptotic factor Bax was increased, the expression levels of caspase-3 and caspase-9 were increased, and the ratio of Bax/Bcl-2 was significantly increased in the model group ($p < 0.01$ or $p < 0.05$). Compared with the model group, the expression of Bcl-2 was increased, the expression of Bax, caspase-3 and caspase-9 was decreased, and the ratio of Bax/Bcl-2 was significantly decreased in the TZQ-L and TZQ-H groups ($p < 0.01$ or $p < 0.05$).

3.2.6. Mechanism by which TZQ improves cardiac function in HL-MI mice

Finally, we created a figure to expound the mechanism by which TZQ improves cardiac function in HL-MI mice. We found that TZQ may improve cardiac function in HL-MI mice by reducing lipid levels, activating PI3K/AKT signalling pathways and reducing apoptosis (Fig. 13).

4. Discussion

CVD has the highest incidence in the world at present and has a serious impact on national economic development [19]. Myocardial ischaemia, the most common type of cardiovascular disease, is caused by changes in coronary artery circulation or structure. It results in ischaemic necrosis of the heart and irreversible damage to cardiac function [20]. Dyslipidaemia is an important influencing factor in

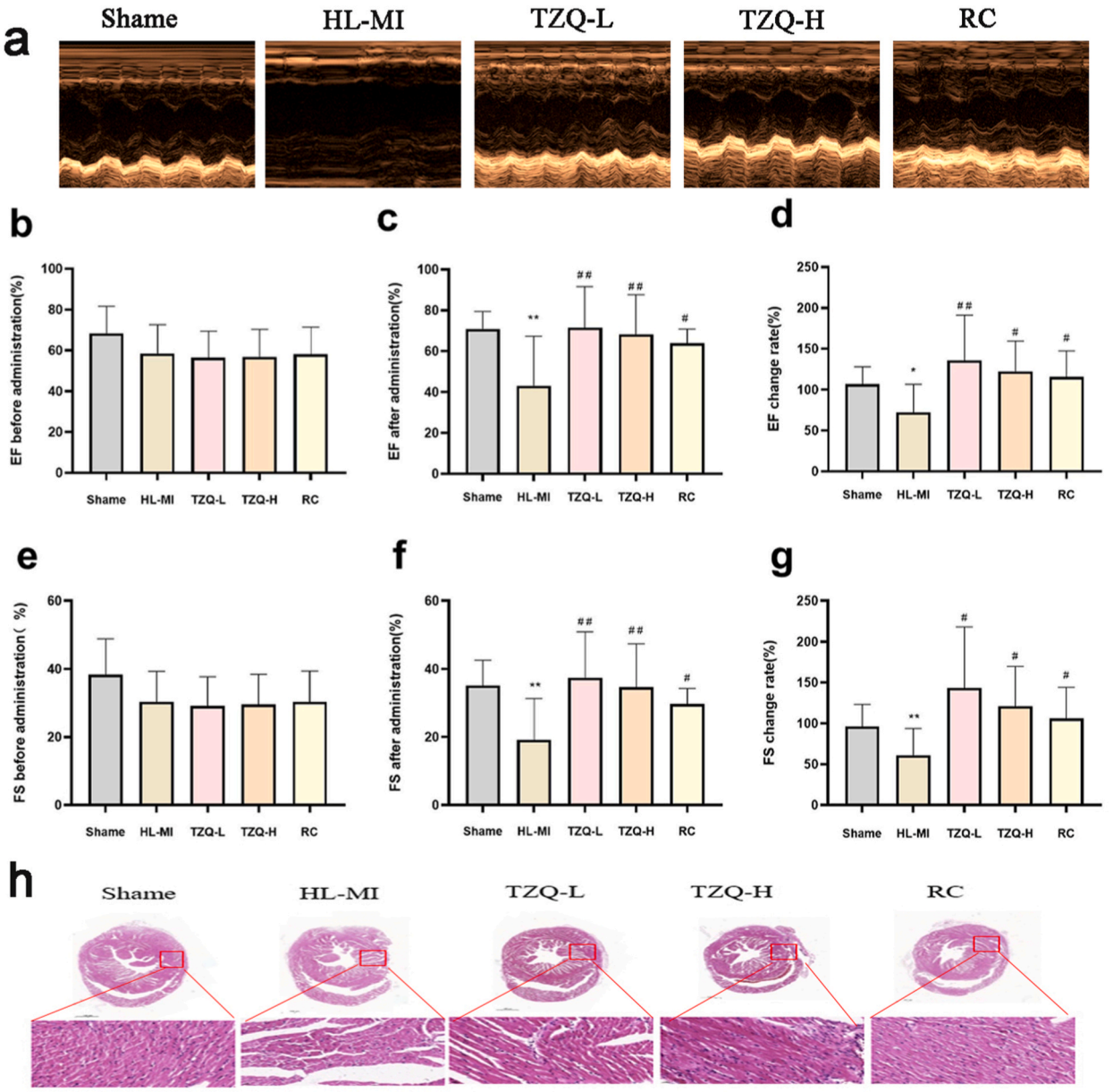

Fig. 10. TZQ improves cardiac function in HL-MI mice. A. Mouse echocardiography **(n = 6)**. B. LVEF after one day of successful myocardial ischaemia modelling **(n = 6)**. C. LVEF six weeks after administration **(n = 6)**. D. The change rate of LVEF in mice before and after administration **(n = 6)**. E. LVFS after one day of successful myocardial ischaemia modelling **(n = 6)**. F. LVFS six weeks after administration **(n = 6)**. H. HE staining of the heart **(n = 3)**. Sham: sham surgery group; HL-MI: model group; TZQ-L: TZQ 6 g/kg group; TZQ-H: TZQ 9 g/kg group; and RC: rosuvastatin 10 mg/kg group. *P < 0.05, **P < 0.01 (compared with sham), $^{\#}P < 0.05$, $^{\#\#}P < 0.01$ (compared with HL-MI).

the incidence of CVD [21,22]. In our study, we found that EF was negatively correlated with TC, TGs, LDL-C, and HDL-C ($P < 0.05$), FS was negatively correlated with TC, TGs, LDL-C, and HDL-C ($P < 0.05$), and the EF change rate and FS change rate were negatively correlated with TGs ($P < 0.05$). Studies have shown that hyperlipidaemia inhibits cardiac autophagy by activating the mTOR signalling pathway and promotes the expression of the apoptosis marker cleaved caspase-3, thus causing irreversible damage to the heart [23,24]. In addition, rats fed a high-fat diet had cardiac and vascular dysfunction, such as myocardial fibrosis, endothelial dysfunction and left ventricular diastolic dysfunction [25]. Studies have also shown increased hydrolysis of adenosine monophosphate (AMP), adenosine triphosphate (ATP), and adenosine diphosphate (ADP) in platelets in hyperlipidaemic rats. In the heart, decreased adenosine production and increased metabolism indicate an impaired response to injury [26]. In rat models of autoimmune myocarditis, hyperlipidaemia increased the expression of the proapoptotic factors caspase-3, Fas and Bax and decreased the expression of the antiapoptotic protein Bcl-2, thereby affecting the structure and function of the heart [27]. However, hyperlipidaemia increases the

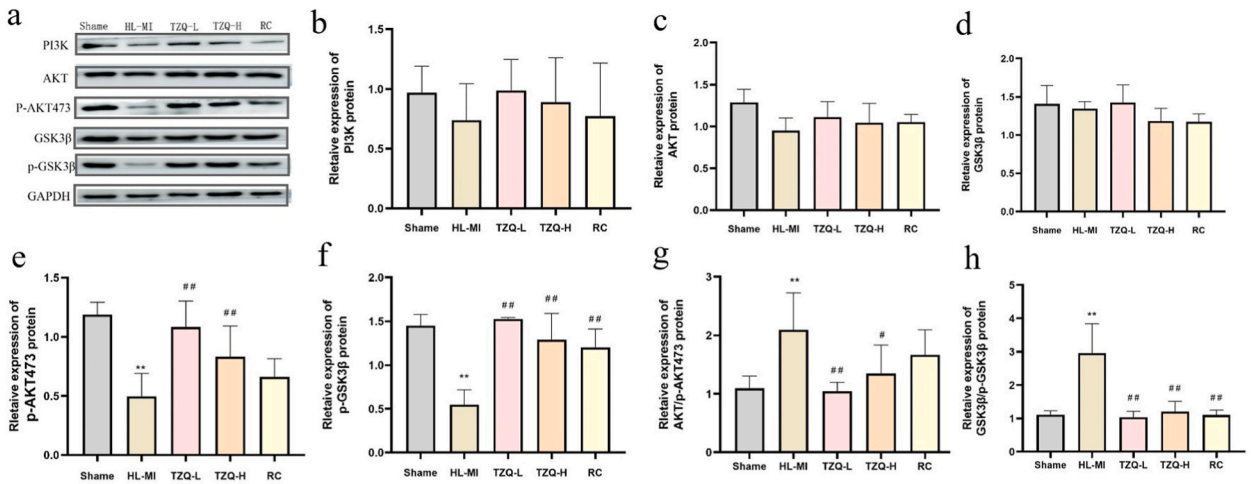

Fig. 11. TZQ improves cardiac function in HL-MI mice by activating the PI3K/AKT signalling pathway (n = 3). A. Expression of PI3K/AKT pathway-related proteins in heart tissue. B. The protein expression levels of PI3K. C. The protein expression levels of AKT. D. The protein expression levels of GSK3β. E. The protein expression levels of p-AKT473. F. The protein expression levels of p-GSK3β. G. Expression of AKT/p-AKT473. H. Expression of GSK3β/p-GSK3β. Sham: sham surgery group; HL-MI: model group; TZQ-L: TZQ 6 g/kg group; TZQ-H: TZQ 9 g/kg group; and RC: rosuvastatin 10 mg/kg group. *P < 0.05, **P < 0.01 (compared with sham), $^{\#}P < 0.05$, $^{\#\#}P < 0.01$ (compared with HL-MI).

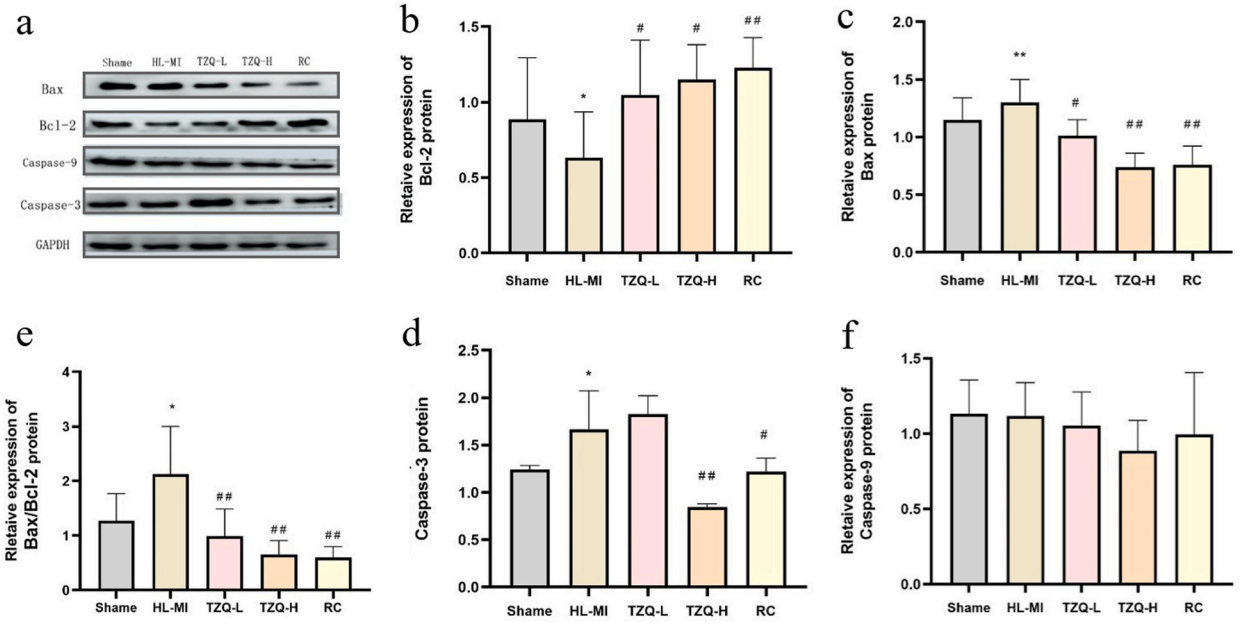

Fig. 12. TZQ improves cardiac function in HL-MI mice by inhibiting apoptosis (n = 3). A. The expression levels of apoptosis-associated proteins in mouse myocardium, as detected by WB. B. The protein expression levels of Bcl-2. C. The protein expression levels of Bax. E. The protein expression levels of Bax/Bcl-2. D. The protein expression levels of caspase-3. F. The protein expression levels of caspase-9. Sham: sham surgery group; HL-MI: model group; TZQ-L: TZQ 6 g/kg group; TZQ-H: TZQ 9 g/kg group; and RC: rosuvastatin 10 mg/kg group. *P < 0.05, **P < 0.01 (compared with sham), $^{\#}P < 0.05$, $^{\#\#}P < 0.01$ (compared with HL-MI).

content of FFAs. This directly leads to lipid disorders in the heart, which stimulates systemic oxidative stress and the inflammatory response. This promotes myocardial interstitial fibrosis and causes the loss of too much troponin I, thereby damaging the heart [28,29]. In addition, hyperlipidaemia directly affects myocardial enzymes, such as Na^{+}-K^{+} ATP, to affect myocardial contractility and cardiac conductivity [5,30]. Most importantly, fatty acid metabolism under physiological conditions is the primary source of energy for the heart [31]. Excess lipid accumulation can affect not only the normal energy supply of the heart [32] but also normal mitochondrial function [33,34]. In summary, lipid-lowering therapy is crucial in the prevention and treatment of cardiovascular disease. The above data are sufficient to prove that TZQ, which can simultaneously reduce lipids and improve cardiac function, is worthy of clinical

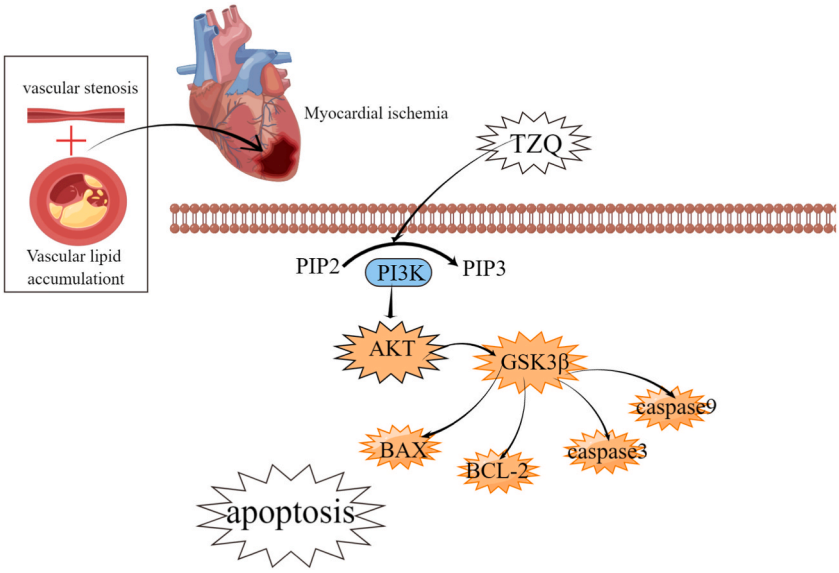

Fig. 13. Mechanism of TZQ in improving cardiac function in HL-MI mice. HL-MI: high-fat diet feeding for 20 weeks to induce hyperlipidaemia combined with left anterior descending coronary artery ligation; TZQ, Tangzhiqing; PI3K, phosphatidylinositol-3-kinase; AKT, protein kinase B; GSK3β, glycogen synthase kinase-3; TC, total cholesterol; TG, triglyceride; LDL-C, low-density lipoprotein cholesterol; HDL-C, high-density lipoprotein cholesterol.

application. The mechanism of action of TZQ will be described in detail below.

Through network analysis, we speculated that TZQ may improve cardiac function by activating the PI3K/AKT signalling pathway and reducing apoptosis. Subsequently, we verified the PI3K/AKT signalling pathway members and apoptosis-related target proteins in animals, such as GSK3β, Bax, Bcl-2, caspase-3, and caspase-9. This strategy demonstrated the accuracy of the network pharmacology predictions. Therefore, we summarized compounds related to PI3K, AKT, GSK3β, Bax, Bcl-2, caspase-3, and caspase-9. By network analysis, seven components were identified as key components of the effect of TZQ against HL-MI (beta-sitosterol, quercetin, kaempferol, tanshinone IIA, tanshinone VI, baicalein, and beta-carotene). Eighteen compounds are related to the above targets. However, they are only associated with one target, so they were not used as key targets (as shown in Table 3). Beta-sitosterol is a common ingredient of red peony and mulberry leaves and is beneficial in treating hyperlipidaemia. Seventy-two patients with hyperlipidaemia had significantly reduced serum TC, LDL and TG levels after oral administration of beta-sitosterol [35]. Quercetin is a common ingredient of mulberry leaves, lotus leaves, and hawthorn leaves. It can not only regulate blood lipids but also improve heart function. Quercetin can improve cardiac function after myocardial ischaemia, myocardial infarction, and myocardial ischaemia–reperfusion in various ways [36–38]. Quercetin significantly improves the acceptability of cholesterol in plasma and HDL and significantly reduces MDA in plasma. Its mechanism of action may be related to the increased expression levels of reverse cholesterol transport-related proteins, such as ATP-binding cassette (ABC) A1 and G1. Kaempferol is a common ingredient of mulberry leaves, lotus leaves, and hawthorn leaves. Kaempferol is a dietary flavonoid that has antiapoptotic, anti-inflammatory and antioxidant effects. A study demonstrated that kaempferol attenuates apoptosis, oxidative stress and inflammation in IR-injured myocardium via the downregulation of p38/JNK and upregulation of ERK1/ERK2 pathway activity [39]. Furthermore, concurrent studies have shown that kaempferol improves insulin sensitivity, inhibits hepatic gluconeogenesis, and regulates the AKT signalling pathway to inhibit lipid accumulation [40–42]. Tanshinone is the main active ingredient of salvia, and its combined effects are free radical scavenging and antioxidant [43,44], anti-inflammatory [45], antiatherosclerotic [46], antifibrotic and antiapoptotic effects. Thus, it prevents ventricular remodelling to maintain normal cardiac function [47]. Tanshinone IIA can inhibit platelet aggregation, improve blood viscosity and exert anticoagulant effects [48]; it also reduces liver lipid buildup, inhibits apoptosis of hepatocytes, and protects the liver by activating PPAR-γ and downregulating TLR4 to exert antioxidant stress and anti-inflammatory effects [49,50]. Baicalein is the main active ingredient of red peony. It has been widely used in the treatment of cardiovascular disease. It can protect the heart through anti-inflammatory, antioxidative stress, and antiapoptotic effects. It can regulate Ca2+ homeostasis by L-type Ca2+ channels and activate the AKT signalling pathway [51–54]. Beta-carotene is the main active ingredient of mulberry leaves. A study found that moderate and low doses of beta-carotene have a certain protective effect on the heart, but high doses of beta-carotene may aggravate heart damage [55,56]. Previous research has shown that beta-carotene can lower serum cholesterol levels while increasing faecal cholesterol levels [57]. Overall, by combining network analysis with animal experiments, we speculate that TZQ could improve cardiac function in HL-MI mice. However, further verification is needed.

To explore the mechanism of action of TZQ in the treatment of HL-MI, this paper combines network analysis with animal experiments. Through network analysis, we speculated that TZQ may improve cardiac function by activating the PI3K/AKT signalling pathway. C57BL/6 mice were fed a high-fat diet for 20 weeks, and the left anterior descending coronary artery was coarctated to form

the HL-MI model. Subsequently, we verified the PI3K/AKT signalling pathway to confirm the network pharmacology prediction. Our animal experiment results showed that TZQ increased the expression of PI3K, AKT, p-AKT, GSK-3β and p-GSK-3β, suggesting that TZQ may improve cardiac function in HL-MI mice through the PI3K/AKT signalling pathway. Studies have shown that the activation of the PI3K/AKT signalling pathway can affect the survival, proliferation and apoptosis of cardiomyocytes, the energy metabolism and regulation of cardiomyocytes, and the regeneration of blood vessels, which is closely related to the regulation of cardiomyocyte function [58]. A recent study showed that Yiqi-Tongluo capsules might alleviate myocardial ischaemia by increasing the phosphorylation of PI3K, Akt and Bcl-2 and decreasing the expression of cleaved caspase-3 and Bax [59]. Polygonum cuspidatum exerts a potent antihyperlipidaemic effect by activating the PI3K/AKT signalling pathway [60]. GSK-3 is a multifunctional serine/threonine protein kinase that exists mainly in the forms of GSK-3α and GSK-3β. GSK-3β is an important molecular signal downstream of AKT [61]. Zhi-Qing Chen et al. proved that breviscapine pretreatment decreased myocardial inflammation and apoptosis in rats after coronary microembolization by activating the PI3K/Akt/GSK-3β signalling pathway [62]. Next, we experimentally verified the apoptosis-related proteins (Bax, Bcl-2, caspase-3, caspase-9) predicted by network pharmacology. In this experiment, the expression of the antiapoptotic factor Bcl-2 was significantly increased after treatment with TZQ administration. Additionally, the expression of Bax, caspase-3 and caspase-9 was significantly reduced, and the ratio of Bcl-2/Bax was significantly increased. These findings are sufficient for explaining the antiapoptotic effect of TZQ. Apoptosis is very important in myocardial ischaemia, as it can initially lead to local cell death and necrosis in the ischaemic region and can then lead to myocardial infarction with an increase in the ischaemic area. This can then develop into heart failure, thereby affecting the overall function and structure of the heart [19,63]. The antiapoptotic factor Bcl-2 and proapoptotic factor Bax are considered to be key influencing factors of apoptosis, and the imbalance in the Bcl-2/Bax ratio is the decisive factor for apoptosis [64,65]. The caspase family is an important family involved in maintaining cell homeostasis and apoptosis and is divided into proapoptotic and proinflammatory members. Caspase-3 and caspase-9 belong to the proapoptotic caspase family. Caspase-3 belongs to the effector family. It can directly degrade intracellular structures and proteins to cause apoptosis and is an important detection index for apoptosis [66]. Caspase-9 is a promoter and participates in the apoptosis process after activation [67]. Xinmailong exerts protective effects against myocardial injury by increasing the expression of Bcl-2 and decreasing the expression of Bax [68]. Trimetazidine can increase myocardial function by decreasing the expression of apoptotic proteins, such as Bax and caspase-3, and reducing myocardial infarct size [69].

Furthermore, although this study has shown that TZQ improves cardiac function in HL-MI mice, the precise type of apoptosis (endothelial cells, cardiomyocytes, macrophages, or smooth muscle cells) is ambiguous. Second, targets related to lipid metabolism in the PI3K/AKT signalling pathway have not been verified in this paper. Finally, we did not personally test the TZQ active ingredients by HPLC or UPLC but cited the early research results of the research group. Far more research is required to improve this situation.

In summary, the results of network analysis and experimental verification in this study indicated that TZQ may improve cardiac function in HL-MI mice by activating PI3K/AKT signalling pathways, reducing lipid levels and reducing apoptosis.

Author contribution statement

Zhihui Song: Conceived and designed the experiments; Performed the experiments; Analyzed and interpreted the data; Wrote the paper.

Rui Chen: Conceived and designed the experiments; Performed the experiments; Wrote the paper.

Caijun Wang, Guiyun Pan, An Yan, Guinan Xie, Wanying Feng: Performed the experiments; Analyzed and interpreted the data.

Zhihua Yang: Analyzed and interpreted the data; Wrote the paper.

Yi Wang: Conceived and designed the experiments; Contributed reagents, materials, analysis tools or data; Wrote the paper.

Data availability statement

No data was used for the research described in the article.

Declaration of interest's statement

The authors declare no conflict of interest.

Ethics statement

The animal study was reviewed and approved by the Medical Ethics Committee of Tianjin University of Traditional Chinese Medicine.

Funding sources

This work was supported by the Innovation Team and Talents Cultivation Program of National Administration of Traditional Chinese Medicine (No: ZYYCXTD-C-202203).

Publisher's note

All claims expressed in this article are solely those of the authors and do not necessarily represent those of their affiliated organizations or those of the publisher, the editors and the reviewers. Any product that may be evaluated in this article or claim that may be made by its manufacturer is not guaranteed or endorsed by the publisher.

Acknowledgements

Thanks to Rui Chen and others for their help in raising the animals. Thanks to Guiyun Pan et al. for assisting in statistical experimental results. Thanks to Wanying Feng et al. for assisting in writing the paper, and thanks to supervisor Yi Wang for guiding the experiment throughout the process, checking the quality, and revising the paper.

Appendix A. Supplementary data

Supplementary data to this article can be found online at https://doi.org/10.1016/j.heliyon.2023.e15645.

References

[1] H. Sun, et al., Global, regional and national burden of non-Hodgkin lymphoma from 1990 to 2017: estimates from global burden of disease study in 2017, Ann. Med. 54 (1) (2022) 633–645.
[2] Guiping Ma, Yiyi Zhang, Research progress in Chinese medicine treatment of hyperlipidemia, J. Integ. Med. Cardiovas. Dise. 17 (14) (2019) 2116–2119.
[3] C. Yan, Z. Xu, W. Huang, Cellular senescence affects cardiac regeneration and repair in ischemic heart disease, Aging Dis. 12 (2) (2021) 552–569.
[4] S. Qin, et al., Instant dark tea alleviates hyperlipidaemia in high-fat diet-fed rat: from molecular evidence to redox balance and beyond, Front. Nutr. 9 (2022), 819980.
[5] Y.S. Yao, T.D. Li, Z.H. Zeng, Mechanisms underlying direct actions of hyperlipidemia on myocardium: an updated review, Lipids Health Dis. 19 (1) (2020) 23.
[6] D.A. Fruman, et al., The PI3K pathway in human disease, Cell 170 (4) (2017) 605–635.
[7] R. Chen, et al., Tongmai Yangxin pill reduces myocardial No-reflow via endothelium-dependent NO-cGMP signaling by activation of the cAMP/PKA pathway, J. Ethnopharmacol. 267 (2021), 113462.
[8] D. Wang, et al., Plasma metabolomics-based reveals the treatment mechanism of ShenGui capsule for application to coronary heart disease in a rat model, Anal. Biochem. 642 (2022), 114480.
[9] X.L. Wu, et al., Rapid characterization of the absorbed chemical constituents of Tangzhiqing formula following oral administration using UHPLC-Q-TOF-MS, J. Separ. Sci. 41 (5) (2018) 1025–1038.
[10] Y. Yan, et al., Study on the mechanism of trefoil glycolipid in treatment of type 2 diabetes mellitus based on network pharmacology, Tianjin Trad. Chin. Med. 37 (4) (2020) 462–468.
[11] J. Nan Xia, et al., Regulation effects of TZQ-F on adipocyte differentiation and insulin action, J. Ethnopharmacol. 150 (2) (2013) 692–699.
[12] J. Gao, et al., Increasing effect of Tangzhiqing formula on IRS-1-dependent PI3K/AKT signaling in muscle, BMC Compl. Alternative Med. 14 (2014) 198.
[13] X. Wang, et al., Effect of tang zhi qing granule on expression of Bax and bcl-2 in myocardium of rats with type 2 diabetes mellitus, J. Tradit. Chin. Med. 29 (12) (2014) 1733–1735.
[14] R. Chen, et al., Integrated pyroptosis measurement and metabolomics to elucidate the effect and mechanism of tangzhiqing on atherosclerosis, Front. Physiol. 13 (2022), 937737.
[15] S. Wang, et al., Study on the regulatory mechanism and experimental verification of icariin for the treatment of ovarian cancer based on network pharmacology, J. Ethnopharmacol. 262 (2020), 113189.
[16] R. Zhang, et al., Network pharmacology databases for traditional Chinese medicine: review and assessment, Front. Pharmacol. 10 (2019) 123.
[17] J. Xu, J. Stevenson, Drug-like index: a new approach to measure drug-like compounds and their diversity, J. Chem. Inf. Comput. Sci. 40 (5) (2000) 1177–1187.
[18] Z. Li, et al., Nuciferine and paeoniflorin can be quality markers of Tangzhiqing tablet, a Chinese traditional patent medicine, based on the qualitative, quantitative and dose-exposure-response analysis, Phytomedicine 44 (2018) 155–163.
[19] B. Zheng, et al., Mechanisms of cinnamic aldehyde against myocardial ischemia/hypoxia injury in vivo and in vitro: involvement of regulating PI3K/AKT signaling pathway, Biomed. Pharmacother. 147 (2022), 112674.
[20] B.R. Pagliaro, et al., Myocardial ischemia and coronary disease in heart failure, Heart Fail. Rev. 25 (1) (2020) 53–65.
[21] D. Zhao, et al., Epidemiology of cardiovascular disease in China: current features and implications, Nat. Rev. Cardiol. 16 (4) (2019) 203–212.
[22] Y. Lu, et al., Comparison of prevalence, awareness, treatment, and control of cardiovascular risk factors in China and the United States, J. Am. Heart Assoc. 7 (3) (2018).
[23] Z. Giricz, et al., Hypercholesterolemia downregulates autophagy in the rat heart, Lipids Health Dis. 16 (1) (2017) 60.
[24] H.C. Hsu, et al., High-fat diet induces cardiomyocyte apoptosis via the inhibition of autophagy, Eur. J. Nutr. 55 (7) (2016) 2245–2254.
[25] S. Watanabe, et al., A high-fat and high-cholesterol diet induces cardiac fibrosis, vascular endothelial, and left ventricular diastolic dysfunction in SHRSP5/Dmcr rats, J. Atherosclerosis Thromb. 25 (5) (2018) 439–453.
[26] A.G. Manzoni, et al., Purine metabolism in platelets and heart cells of hyperlipidemic rats, Cardiovasc. Drugs Ther. 34 (6) (2020) 813–821.
[27] H. Chang, et al., Cardiac apoptosis caused by elevated cholesterol level in experimental autoimmune myocarditis, Exp. Cell Res. 395 (1) (2020), 112169.
[28] Q. Han, et al., Dysregulation of cardiac lipid parameters in high-fat high-cholesterol diet-induced rat model, Lipids Health Dis. 17 (1) (2018) 255.
[29] Y. Cheng, et al., Large accumulation of collagen and increased activation of mast cells in hearts of mice with hyperlipidemia, Arq. Bras. Cardiol. 109 (5) (2017) 404–409.
[30] H.K. Saini, A.S. Arneja, N.S. Dhalla, Role of cholesterol in cardiovascular dysfunction, Can. J. Cardiol. 20 (3) (2004) 333–346.
[31] T. Doenst, T.D. Nguyen, E.D. Abel, Cardiac metabolism in heart failure: implications beyond ATP production, Circ. Res. 113 (6) (2013) 709–724.
[32] N. Cheng, et al., Crucial role of mammalian glutaredoxin 3 in cardiac energy metabolism in diet-induced obese mice revealed by transcriptome analysis, Int. J. Biol. Sci. 17 (11) (2021) 2871–2883.
[33] P. Mishra, D.C. Chan, Metabolic regulation of mitochondrial dynamics, J. Cell Biol. 212 (4) (2016) 379–387.
[34] A. Yan, et al., Effects of lipid overload on heart in metabolic diseases, Horm. Metab. Res. 53 (12) (2021) 771–778.
[35] S. Devaraj, I. Jialal, S. Vega-López, Plant sterol-fortified orange juice effectively lowers cholesterol levels in mildly hypercholesterolemic healthy individuals, Arterioscler. Thromb. Vasc. Biol. 24 (3) (2004) e25–e28.
[36] S.S. El-Sayed, et al., Quercetin ameliorated remote myocardial injury induced by renal ischemia/reperfusion in rats: role of Rho-kinase and hydrogen sulfide, Life Sci. 287 (2021), 120144.

[37] L.Y. Dong, et al., Quercetin attenuates myocardial ischemia-reperfusion injury via downregulation of the HMGB1-TLR4-NF-κB signaling pathway, Am. J. Trans. Res. 10 (5) (2018) 1273–1283.
[38] J. Tang, et al., Quercetin improve ischemia/reperfusion-induced cardiomyocyte apoptosis in vitro and in vivo study via SIRT1/PGC-1α signaling, J. Cell. Biochem. 120 (6) (2019) 9747–9757.
[39] K. Suchal, et al., Kaempferol attenuates myocardial ischemic injury via inhibition of MAPK signaling pathway in experimental model of myocardial ischemia-reperfusion injury, Oxid. Med. Cell Longev. 2016 (2016), 7580731.
[40] B. Lee, et al., Kaempferol isolated from Nelumbo nucifera inhibits lipid accumulation and increases fatty acid oxidation signaling in adipocytes, J. Med. Food 18 (12) (2015) 1363–1370.
[41] H. Alkhalidy, et al., Kaempferol ameliorates hyperglycemia through suppressing hepatic gluconeogenesis and enhancing hepatic insulin sensitivity in diet-induced obese mice, J. Nutr. Biochem. 58 (2018) 90–101.
[42] T. Wang, Q. Wu, T. Zhao, Preventive effects of kaempferol on high-fat diet-induced obesity complications in C57BL/6 mice, BioMed Res. Int. 2020 (2020), 4532482.
[43] A.H. Fei, et al., Salvianolate inhibits reactive oxygen species production in H(2)O(2)-treated mouse cardiomyocytes in vitro via the TGFβ pathway, Acta Pharmacol. Sin. 34 (4) (2013) 496–500.
[44] B. Han, et al., Protective effects of salvianolate on microvascular flow in a porcine model of myocardial ischaemia and reperfusion, Arch. Cardiovas. Dis. 104 (5) (2011) 313–324.
[45] C. Meng, et al., Protection of salvianolate against atherosclerosis via regulating the inflammation in rats, J. Huazh. Univ. Sci. Techn. Med. Sci. 34 (5) (2014) 646–651.
[46] D. Zhao, et al., Tanshinone II A stabilizes vulnerable plaques by suppressing RAGE signaling and NF-κB activation in apolipoprotein-E-deficient mice, Mol. Med. Rep. 14 (6) (2016) 4983–4990.
[47] D.M. Wu, et al., Tanshinone IIA prevents left ventricular remodelling via the TLR4/MyD88/NF-κB signalling pathway in rats with myocardial infarction, J. Cell Mol. Med. 22 (6) (2018) 3058–3072.
[48] F. Maione, et al., Tanshinone IIA, a major component of Salvia milthorriza Bunge, inhibits platelet activation via Erk-2 signaling pathway, J. Ethnopharmacol. 155 (2) (2014) 1236–1242.
[49] L. Huang, et al., Tanshinone IIA ameliorates non-alcoholic fatty liver disease through targeting peroxisome proliferator-activated receptor gamma and toll-like receptor 4, J. Int. Med. Res. 47 (10) (2019) 5239–5255.
[50] M.A. Ansari, et al., Prospective therapeutic potential of Tanshinone IIA: an updated overview, Pharmacol. Res. 164 (2021), 105364.
[51] J. Li, et al., Baicalein ameliorates myocardial ischemia through reduction of oxidative stress, inflammation and apoptosis via TLR4/MyD88/MAPK(S)/NF-κB pathway and regulation of Ca(2+) homeostasis by L-type Ca(2+) channels, Front. Pharmacol. 13 (2022), 842723.
[52] X. Wang, et al., Baicalein alleviates pyroptosis and inflammation in hyperlipidemic pancreatitis by inhibiting NLRP3/Caspase-1 pathway through the miR-192-5p/TXNIP axis, Int. Immunopharm. 101 (Pt B) (2021), 108315.
[53] J. Li, et al., Baicalein preventive treatment confers optimal cardioprotection by PTEN/Akt/NO activation, Am. J. Chin. Med. 45 (5) (2017) 987–1001.
[54] Q. Li, et al., Baicalein inhibits mitochondrial apoptosis induced by oxidative stress in cardiomyocytes by stabilizing MARCH5 expression, J. Cell Mol. Med. 24 (2) (2020) 2040–2051.
[55] E. Csepanyi, et al., Cardiovascular effects of low versus high-dose beta-carotene in a rat model, Pharmacol. Res. 100 (2015) 148–156.
[56] E. Csepanyi, et al., Beta-carotene affects the effects of heme oxygenase-1 in isolated, ischemic/reperfused rat hearts: potential role of the iron, Molecules 27 (9) (2022).
[57] L.S. Silva, et al., Diet supplementation with beta-carotene improves the serum lipid profile in rats fed a cholesterol-enriched diet, J. Physiol. Biochem. 69 (4) (2013) 811–820.
[58] L. Yang, N. Wang, Y. Liu, Research progress of PI3K/Akt signaling pathway regulating cardiac function, Heart J. 30 (3) (2018) 344–347.
[59] H. Duan, et al., An integrated approach based on network analysis combined with experimental verification reveals PI3K/Akt/Nrf2 signaling is an important way for the anti-myocardial ischemia activity of Yi-Qi-tong-Luo capsule, Front. Pharmacol. 13 (2022), 794528.
[60] T. Tao, et al., Polygonum cuspidatum extract exerts antihyperlipidemic effects by regulation of PI3K/AKT/FOXO3 signaling pathway, Oxid. Med. Cell. Longev. 2021 (2021), 3830671.
[61] X. Han, et al., Buyang Huanwu Decoction promotes angiogenesis in myocardial infarction through suppression of PTEN and activation of the PI3K/Akt signalling pathway, J. Ethnopharmacol. 287 (2022), 114929.
[62] Z.Q. Chen, et al., Breviscapine pretreatment inhibits myocardial inflammation and apoptosis in rats after coronary microembolization by activating the PI3K/Akt/GSK-3β signaling pathway, Drug Des. Dev. Ther. 15 (2021) 843–855.
[63] L. Zhu, et al., The cardioprotective effect of salidroside against myocardial ischemia reperfusion injury in rats by inhibiting apoptosis and inflammation, Apoptosis 20 (11) (2015) 1433–1443.
[64] C. Yi, et al., Asiatic acid alleviates myocardial ischemia-reperfusion injury by inhibiting the ROS-mediated mitochondria-dependent apoptosis pathway, Oxid. Med. Cell. Longev. 2022 (2022), 3267450.
[65] H. Flores-Romero, et al., BCL-2-family protein tBID can act as a BAX-like effector of apoptosis, EMBO J. 41 (2) (2022) e108690.
[66] C.D. Buckley, et al., RGD peptides induce apoptosis by direct caspase-3 activation, Nature 397 (6719) (1999) 534–539.
[67] C. Rogers, et al., Cleavage of DFNA5 by caspase-3 during apoptosis mediates progression to secondary necrotic/pyroptotic cell death, Nat. Commun. 8 (2017), 14128.
[68] L. Jin, et al., Putative prevention of XML injection against myocardial ischemia is mediated by PKC and PLA2 proteins, Front. Cell Dev. Biol. 10 (2022), 827691.
[69] Z. Wu, et al., Protective mechanism of trimetazidine in myocardial cells in myocardial infarction rats through ERK signaling pathway, BioMed Res. Int. 2021 (2021), 9924549.